Domain-Size Effects in Optical Diffraction from Polymer/Composite Microparticles

Jess V. Ford, Bobby G. Sumpter, Donald W. Noid, and Michael D. Barnes*

Chemical and Analytical Sciences Division, MS 6142, Oak Ridge National Laboratory, Oak Ridge, Tennessee 37831-6142

Steven C. Hill and David B. Hillis

Army Research Laboratory, 2800 Powder Mill Road, Adelphi, Maryland 20783-1197

Received: August 11, 1999; In Final Form: November 17, 1999

Poly(ethylene glycol) [PEG] microparticles were doped with ceramic or latex nanoparticles in order to examine domain-size and refractive index effects of nanometer-sized guest inclusions on two-dimensional diffraction patterns. Composite microparticles were examined for different inclusion sizes and polymer/nanoparticle weight ratios in order to determine the size and number-density threshold of detection for guest nanoparticles within the polymer host as indicated by fringe distortion in 2-D angular scattering. PEG host particles having a 10 μm (nominal) diameter were formed with three different guest nanoparticles (Al_2O_3, TiO_2, and latex nanospheres with respective sizes of 46, 29, and 14 nm). For the ceramic nanoparticle inclusions, distortion was observed at relative guest−host weight fractions of 5−10%. For the 14 nm latex inclusions, no distortion was observed at any weight fraction. A perturbation method was used to simulate the effect of nanometer-size inclusions on 2-D optical diffraction from polymer host microparticles and to suggest how the distortions should vary with inclusion size, refractive index, and number.

Introduction

Synthesis of polymer/polymer and polymer/inorganic composites has attracted a great deal of attention as a method of producing nanoscale alloys with tunable properties.[1] As an example, addition of ceramic nanoparticles to poly(ethylene glycol) [PEG]/electrolyte composites has been investigated as a way to suppress phase separation in polymer/salt systems, thereby enhancing conductivity[2] and mechanical properties.[3] Polymer blends and phase separation behavior in mixed polymer and polymer/inorganic systems are also under intense investigation with the ultimate goal of producing "designer" materials on an arbitrary length scale. Recently, we have shown that a microdroplet approach can be used to prepare homogeneous polymer-blend microparticles from bulk-immiscible polymers.[4,5] To characterize these polymer alloy particles, we used 2-D optical diffraction where the presence of phase-separated inclusions was signaled by fringe distortion in measured 2-D diffraction patterns. An important question in assessing the particle homogeneity based on optical diffraction measurements is the inclusion size threshold for producing measurable distortion and how this critical length scale compares with molecular dimensions in mixed polymer systems.

In this paper, we simulate the effects of phase separation in polymer blend microparticles by preparing PEG host microparticles doped with nanoparticles ranging in size from 14 to 46 nm. The purpose of this work was to identify size and number density thresholds for the onset of distortion in 2-D optical diffraction from composite microparticles. The experimental apparatus and method used in the present study have been applied to the detection of single molecules in droplet streams,[6] probing phase separation behavior in polymer blend microparticles, and polymer electrolytes[7] in our laboratory. We showed that two-dimensional optical diffraction from spherical polymer composite particles is a convenient and powerful tool for probing phase separation behavior of mixed polymer systems confined to femtoliter volumes. This approach is similar to the work of Chang and co-workers on two-dimensional angular optical scattering (TAOS) from spheroids and composite particles,[8] but our emphasis has focused on phase separation behavior of mixed polymer systems co-dissolved in droplets of dilute solution. In preliminary work,[4] we showed that fringe distortion provides a qualitative indicator of the presence of phase-separated domains (with different refractive indices). However, because it is a nonimaging technique, the measurement does not provide an obvious measure of phase-separated domain sizes in composite particles. Thus, a central question that arose from that work was how small could the inclusion (or domain size) be and still produce measurable distortion in 2-D diffraction patterns. In this paper we address this issue by mimicking the effects of phase separation by creating heterogeneous particles with known inclusion sizes and refractive indices.

Particle trapping techniques have been used for a number of years to isolate mesoscale objects for detailed optical measurements.[9−13] For microspheres, Mie theory can be used to characterize physical properties of the droplets by comparing the angle-integrated elastic scattering (or fluorescence) intensity and measuring the position of morphology-dependent resonances (MDRs) for slowly evaporating liquid droplets.[14] MDR-mediated phenomena have been observed in a wide variety of optical effects in microparticles such as cavity-modified fluorescence[15−18] and Raman scattering,[19,20] nonlinear optical phenomena,[21] and enhanced energy transfer in liquid microdroplets.[22]

However, for particles that evaporate very slowly or not at all (where the change in size parameter is less than the spacing between MDRs), an MDR-based approach for particle charac-

* To whom correspondence should be addressed. Phone: 865-574-4923. Fax: 865-574-8363. E-mail: nmz@ornl.gov.

10.1021/jp992843m CCC: $19.00
Published on Web 12/28/1999

terization using a fixed wavelength is impractical. Alternatively, the scattering intensity as a function of θ (i.e., the phase function)[23] is also highly sensitive to size and refractive index (both real and imaginary parts) and can be compared quantitatively with Mie theory calculations. With a careful calibration of the detector channel number to a specific scattering angle, the optimal fit of the angular scattering pattern (in one dimension) yields the microparticle size and refractive index with uncertainties of ± 0.005 μm and 5×10^{-4}, respectively, and without aliasing effects.

In this paper, we compare two-dimensional angular scattering (diffraction) patterns from homogeneous (single-component) polymer particles with those obtained from polymer host particles doped with either ceramic or latex nanoparticles. By varying the size and refractive index of the nanoscale dopants, we examined the onset of particle inhomogeneity, which is manifested as a reduction or total loss of fringe contrast in the measured diffraction patterns. Nanoparticles with nominal dimensions of 14, 29, and 46 nm and refractive indices of 1.59, 2.5, and 1.7 were used to test the sensitivity of the method to guest domain size, refractive index, and number density. We show theoretically that domain-size (and refractive index) thresholds for measurable distortion in 2-D diffraction patterns is related to a nanoparticle scattering efficiency,

$$P = \frac{d^3}{\lambda^2}\left|\frac{m^2 - 1}{m^2 + 2}\right|$$

where d is the diameter of the inclusion or subdomain, λ is the probe wavelength, and m is the reduced or relative refractive index defined as n_{guest}/n_{host}.

Experimental Section

In this work, heterogeneous polymer/ceramic and polymer/latex-sphere microparticles were levitated in an electrodynamic trap and interrogated using a vertically polarized HeNe laser (632.8 nm). Details of the experimental apparatus, optical setup, and calibration procedures for correlating CCD pixel to optical scattering angle have been presented elsewhere.[24,25]

Aqueous polymer stock solutions were prepared using PEG with an average molecular weight of 10 000 (PEG 10K) amu (Aldrich) in 250 mL batches at ~1.35 wt %. The polymer ceramic solutions were formulated by mixing a known weight of the stock solution and either γ-Al_2O_3 (Alfa-Æsar) or rutile TiO_2 (Alfa-Æsar) powders. The average particle sizes and refractive indices (real part) for Al_2O_3 and TiO_2 are 46 nm and 29 nm and 1.7 and 2.5, respectively. The average particle sizes, specified by the manufacturer, were based on the specific surface area measurements. The polymer/latex-sphere solution was prepared by mixing the stock solution with a 2% fluorescent dye tagged carboxylated poly(styrene) latex sphere solution (Molecular Probes Inc, L-5473, FluoSphere) with a nominal particle size of 14 nm and a refractive index of ~1.59. All reagents were used without additional purification or drying, and stock solutions were prepared using water generated from a Nanopure (Barnstead/Thermolyne) water system.

Droplets were generated on demand using a piezoelectric droplet generator following loading of the polymer/electrolyte solution in a Pyrex tip through vacuum aspiration. It was observed that over approximately 10 min the ceramic particles at all sample concentrations would sediment to the bottom of the tip and clog the orifice. Therefore, each experimental run was completed using freshly mixed solutions. The tip was cleaned between each experimental run prior to solution loading to ensure that microparticle sizes obtained were consistent for each dopant concentration studied. Prior to droplet generation the electrodynamic trap was flushed with dry nitrogen, ensuring rapid evaporation of solvent. Previous work on pure PEG particles found that flushing the trap with dry nitrogen resulted in trapped microparticles with less than 1% residual water.[7]

The trap utilized has a three-electrode geometry.[12,25] An induction electrode above the trap biased at ~400 V was used to increase the charge-to-mass ratio to improve trapping. A 60 Hz ac potential (~200−500 Vac) was applied to the ring electrode, and the endcaps were biased with a small dc voltage to offset the gravitational force. The scattering angle was $90° \pm 17.5°$ with respect to the laser axis (limited geometrically by the *f*/1.5 collection objective). The collimated light was spatially filtered and reduced in size to match the dimensions of the CCD chip. The CCD (SpectraSource Instruments) was thermoelectrically cooled and digitized at 16 bits. Measured 2-D diffraction patterns were stored, and 1-D horizontal slices corresponding to the 0° polar angle were matched to Mie theory to find the particle size and refractive index that minimized the error parameter associated with the fit.

Results and Discussion

These experiments were undertaken to explore the questions relevant to probing phase-separation behavior in mixed polymer systems, specifically, issues of domain size and refractive index and whether molecular-scale "resolution" could be obtained with angle-resolved light scattering techniques.[26] Particle inhomogeneity was observed to reduce fringe contrast in Fraunhofer diffraction patterns as well as to produce a general distortion in the two-dimensional pattern. These distortions are typically observed as voids in the pattern, non-Gaussian intensity fluctuations along the fringes, formation of islandlike structures, or complete loss of a well-defined vertical fringes.[4] The focus of this work was to examine PEG host microparticles doped with nanoparticles of varying size and refractive index to determine the minimum detectable size and refractive index and number density from the onset of distorted two-dimensional diffraction patterns.

Figure 1 shows surface plots of simulated 2-D diffraction patterns from a host particle doped with 200 (Figure 1A) and 900 (Figure 1B) guest inclusions in an 8 μm host particle. The simulations were computed using a perturbation method to model the scattering by a sphere containing inclusions, called the volume−current method (VCM).[27] Details of the model are presented later in the paper. The simulation was designed to model the experimental measurements on PEG/TiO_2 composite microparticles. The inclusion diameter and refractive index (n_{guest}) was set to 30 nm and 2.5, respectively, and the host sphere diameter and refractive index (n_{host}) were chosen to be 8 μm and 1.47, respectively. Both simulations show similar intensity oscillations along the polar angle, with a slightly higher depth of modulation for the 900-inclusion simulation. The 200-inclusion simulation suggests sensitivity to a relative weight fraction of $\sim 10^{-5}$.

To provide a quantitative comparison with a homogeneous reference, we analyzed the Fourier transforms of intensity fluctuations along the polar angle for individual diffraction fringes. The idea is that intensity oscillations along a single fringe that might be too weak to see on a 2-D gray scale plot might be more readily apparent by comparing Fourier transforms with a homogeneous reference. Figure 2 shows equal area plots of a comparison between polar angle Fourier transforms for a homogeneous particle and 100- and 200-inclusion simulations.

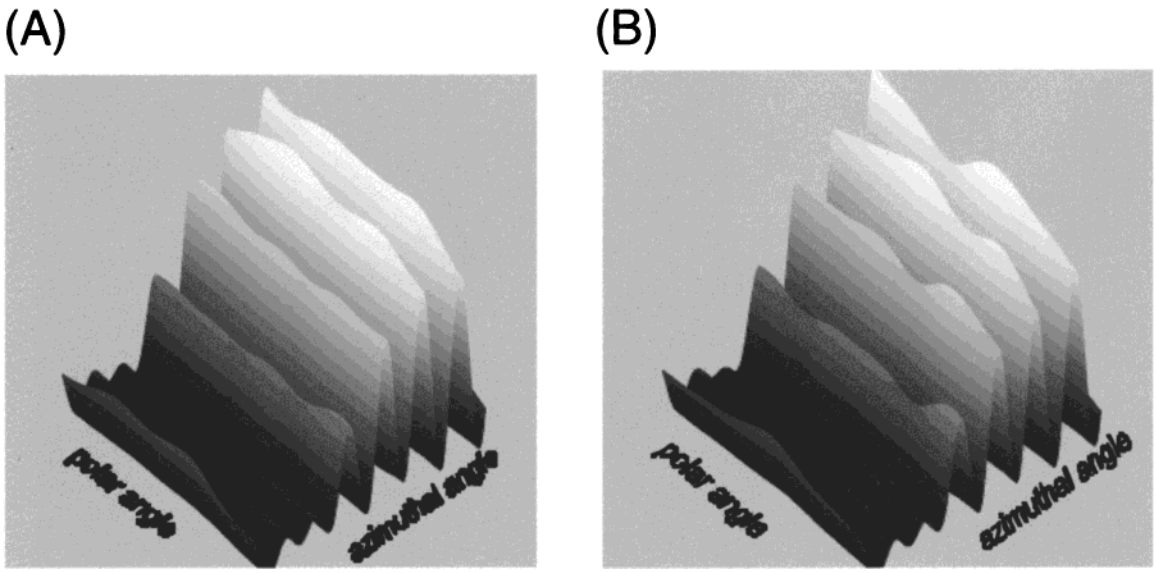

Figure 1. Two-dimensional optical diffraction patterns computed using a VCM simulation for 8 μm host microparticles ($n = 1.46$) doped with (A) 200 and (B) 900 guest nanoparticles with a diameter of 30 nm and a refractive index of 2.5.

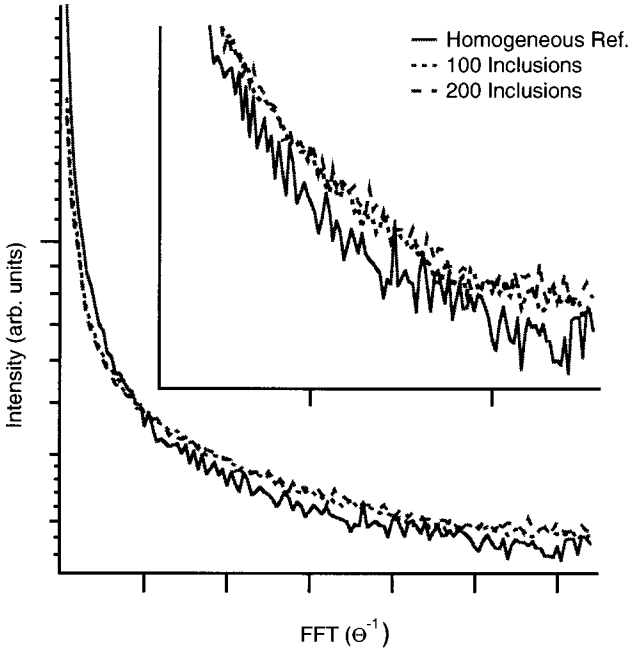

Figure 2. Fourier transforms of scattering intensity along individual fringes (fixed azimuthal angle) from VCM simulations for a homogeneous microparticle (−), a PEG microparticle with 100 guest inclusions (···), and a PEG microparticle with 200 guest inclusions (- - -) at full scale (A) and on an expanded scale (B) to highlight intensity differences away from the center point.

The theoretical simulations clearly indicate that a relatively small number of inclusions, ~200, cause visible distortions in the 2-D optical diffraction pattern obtained and that even 100 inclusions cause small distortions that cause changes in Fourier transforms of vertical fringe intensity. These simulations also illustrate the importance of measuring diffraction resolved on both azimuthal and polar angles; without the information on intensity oscillations along a given fringe, such 1-D diffraction patterns would clearly be interpreted as coming from a homogeneous particle.

Table 1 summarizes the data for the three different PEG/nanoparticle composite systems. The PEG (10K MW) host refractive index was determined to be 1.4717 from a comparison of 1-D experimental scattering data to Mie theory calculations. Figure 3 shows 2-D diffraction data for PEG host microparticles

TABLE 1: Summary of Polymer/Nanoparticle Host/Guest Data

guest inclusion	average size (nm)	n_{guest}	m	P [a] (nm)	concentration threshold for particle inhomogeneity (host/guest wt ratio)
Al_2O_3	46	1.7	1.16	0.026	13:1
TiO2	29	2.5	1.71	0.024	13:1
latex nanospheres	14	1.59	1.09	4×10^{-4}	

[a] P calculated from eq 8 with host refractive index of 1.46.

doped with 46 nm Al_2O_3 particles ($P = 0.026$) with different relative mass fractions. At low guest/host weight fraction ratios (1:85), the presence of alumina nanoparticles did not result in measurable distortion of the diffraction pattern; i.e., the pattern was similar to that for pure PEG, although the refractive index was slightly lower than that of pure PEG (1.465), indicating a significant amount of residual water within the particle. At a relative guest/host mass fraction of 1:13, intensity distortions along the diffraction fringes were easily visible, although well-defined fringes were still present as evidenced by comparison with Mie theory calculations. At higher relative guest−host mass fractions, no discernible diffraction fringes were observed, indicating that the microparticle is clearly inhomogeneous. Figure 4 illustrates the differences in the Mie theory fitting and the vertical fringe contrast between a homogeneous (mass fraction 85:1) and an inhomogeneous (mass fraction of 13:1) PEG microparticle doped with alumina.

Similar observations were made for addition of TiO_2 nanoparticles in PEG host microparticles. Although the particles are smaller, the refractive index (2.5) is significantly higher and the resulting scattering efficiency is nearly the same as for Al_2O_3. Figure 5 shows diffraction patterns obtained for four TiO_2/PEG weight ratios (1:93, 1:13, 1:1, and 7:1). For the smallest TiO_2/PEG weight ratio (1:93), there is no indication of particle inhomogeneity. Similar to results for Al_2O_2, PEG microparticles doped with TiO_2 at a guest/host mass ratio of 1:13 (Figure 5B) have well-defined diffraction fringes, but there are clearly non-Gaussian intensity fluctations along the polar angle. The similarity in dopant concentration threshold for particle homogeneity compared with the Al_2O_3 particles is consistent with the fact that, despite differences in size, the scattering efficien-

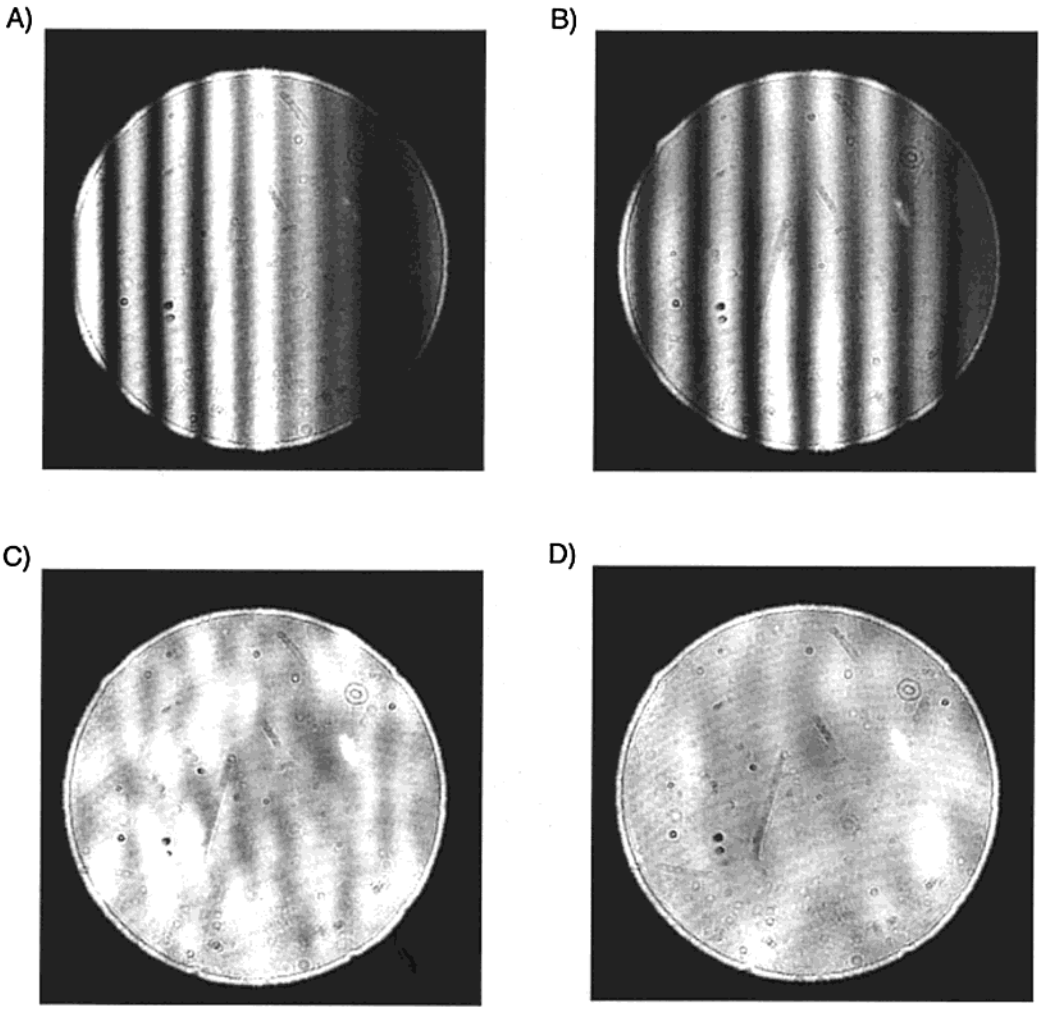

Figure 3. Experimental two-dimensional Fraunhofer diffraction patterns from PEG microparticles doped with Al_2O_3: (A) polymer-to-ceramic (P/C) weight fraction of 85:1; (B) P/C weight fraction of 13:1; (C) P/C weight fraction of 1:1; (D) P/C weight fraction of 1:8.

cies are basically the same for the two types of nanoparticles. At higher TiO_2/PEG weight ratios (Figure 5C), the fringe pattern shows nonuniform vertical fringe intensities and voids, which is an obvious signature of material inhomogeneity. Figure 5D is an excellent illustration of a diffraction pattern where there are a large number of distinct optical domains; there is no discernible fringe pattern.

Figure 6 shows the diffraction pattern from a microparticle of PEG doped with 14 nm carboxylated poly(styrene) latex spheres ($n_{incl} \approx 1.59$) and a 1-D slice of the diffraction pattern taken at the zero polar angle with the Mie theory match to the data. Unlike the ceramic systems, the latex-doped microparticles did not exhibit any measurable distortion in the scattering patterns, even with a polymer-to-particulate weight ratio of ~1:1. This observation implies that the microparticle is homogeneous, which is not surprising because the relative scattering efficiency (P) is considerably smaller than that of either of the ceramic dopants.

Interestingly, the refractive index for the latex/PEG composite particle (1.518) is very close to the value expected from a homogeneous solution of the two materials as determined from procedure given in ref 25, assuming that the microparticle is unaffected by residual solvent and that molar volumes are additive. In contrast, the refractive index for homogeneous PEG/ceramic composite particles lies below the pure PEG value. Since the refractive index of the composite microparticle (~1.46) is lower than that of pure PEG (and much lower than the refractive index of the ceramic), this suggests that doping with low concentrations of ceramic nanoparticles results in the retention of residual solvent. Furthermore, the contribution of the dopant refractive index to the overall microparticle refractive index must therefore be small. However, the higher concentrations of ceramic nanoparticles have refractive indices comparable to or larger than pure PEG, implying that either the residual water content is reduced or, more likely, that contributions to the overall microparticle refractive index from the ceramic nanoparticles have increased.

While it is possible that some aggregation of guest nanoparticles occurs, especially at higher concentrations, we expect that the contribution is negligible (especially at lower doping levels). Any nanoparticle aggregation probably occurs in the base solution before microdroplet ejection into the trap. In an effort to eliminate aggregation in the base solution, the solution was vigorously mixed prior to loading of the droplet generator. Additionally, the likelihood of aggregation occurring during microparticle formation is minimal, since the diffusion of nanoparticulates in microparticles of this size is limited (diffusion coefficient of $\sim 10^{-9}$ cm^2/s) to several particle diameters during the initial 100−200 ms where rapid particle drying occurs. Furthermore, once the microparticle is dry, mobility of the guest nanoparticles in the host polymer matrix is essentially zero. It should be noted that Arnold and co-workers observed aggregation of guest particles at the surface of saturated sodium chloride microdroplets.[28] However, the work presented here

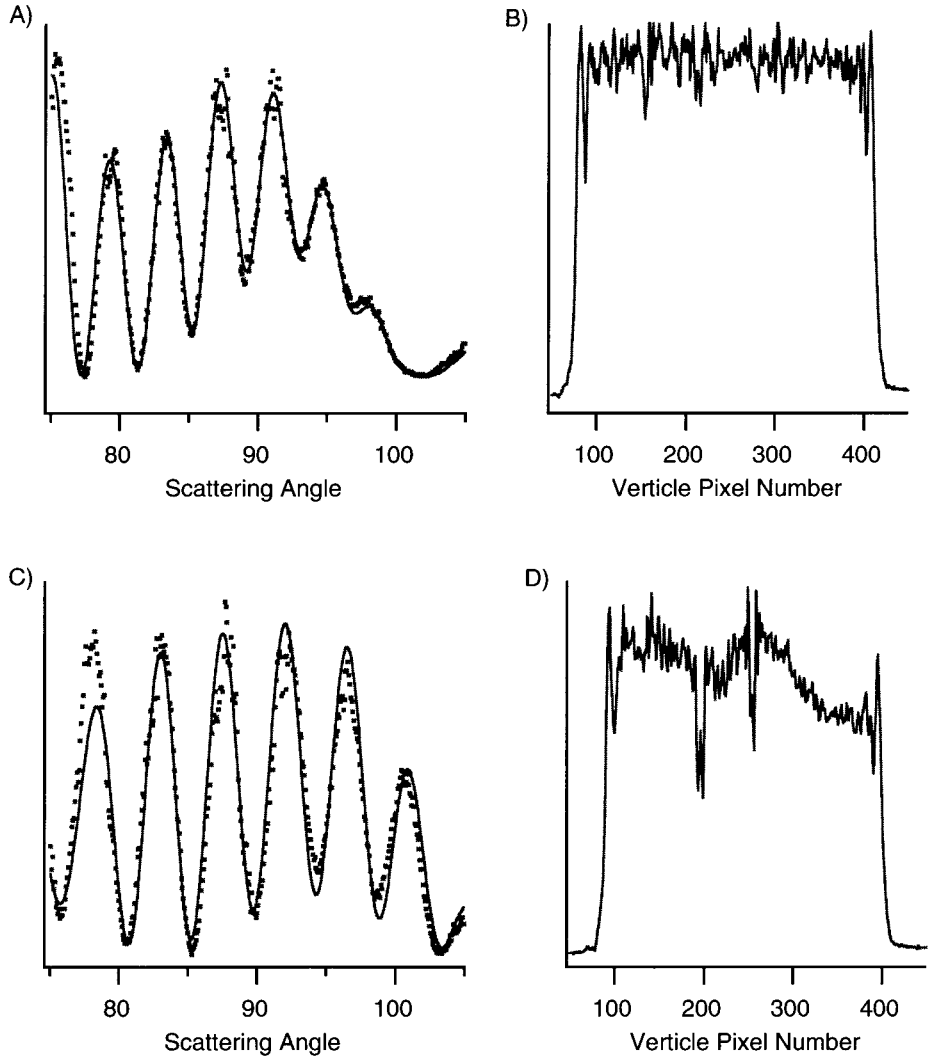

Figure 4. Comparison of 1-D azimuthal scattering with Mie theory matches and corresponding vertical intensity fluctuations along selected individual fringes for typical PEG host microparticles doped at weight fractions of 85:1 (A, B) and 13:1 (C, D) Al_2O_3. Plots A and C illustrate the differences in the Mie theory fits, where the points are the experimental data and the solid line is the theoretical result. Plots B and D illustrate the difference in vertical fringe contrast.

deals with a dry polymeric environment that eliminates diffusion of guest nanoparticles, whereas the previous work on guest inclusions was done using liquid droplets where diffusion plays an important role in determining the location of guest particles within the host droplet.

Volume−Current Method for Simulation of 2-D Diffraction Patterns

In the volume current method (VCM), the internal field at each inclusion is computed assuming the sphere is homogeneous. The additional polarization generated is proportional to the difference between the polarization of the inclusion and the polarization in that volume if the inclusion were not there. This polarization is treated as a radiating source, which emits inside an otherwise homogeneous sphere (the electromagnetic boundary conditions are matched at the surface of the host sphere). The total scattered field at any point is the coherent sum of the scattering from the host sphere (assumed to be homogeneous) and the scattering from all of the inclusions. The method is valid only when the scattering from the inclusions is small enough that the fields scattered by the inclusions at internal points is small compared to the internal fields that would be generated inside a homogeneous sphere. This perturbation method should be appropriate for modeling the first detectable deviations from the scattering patterns of homogeneous spheres.

The VCM differs from simple Rayleigh scattering. If the inclusions were in a bulk medium instead of a microsphere, the optical diffraction patterns could be computed from Rayleigh scattering theory,[29] which is applicable to particles having diameters much smaller than a wavelength. The electric fields scattered from each inclusion particle would be coherently summed before calculating the squared magnitude of the total field to obtain the intensity distribution (assuming the light source has a sufficiently long coherence length).

In the VCM, the inclusions and the host sphere are electromagnetically coupled. In computing the 2-D scattering patterns by inhomogeneous spheres, we used the VCM with the modification for Rayleigh type particles described in section 26 of ref 27, and without the computation of an effective average refractive index. The only difference is that here we compute and show two-dimensional instead of one-dimensional angular distributions. However, because of our interest in the detectability of inclusions as a function the domain parameters (size, refractive index, and number), we examine here in more detail the field and intensity expressions from the VCM to try to understand how the inclusion-dependent scattering intensites

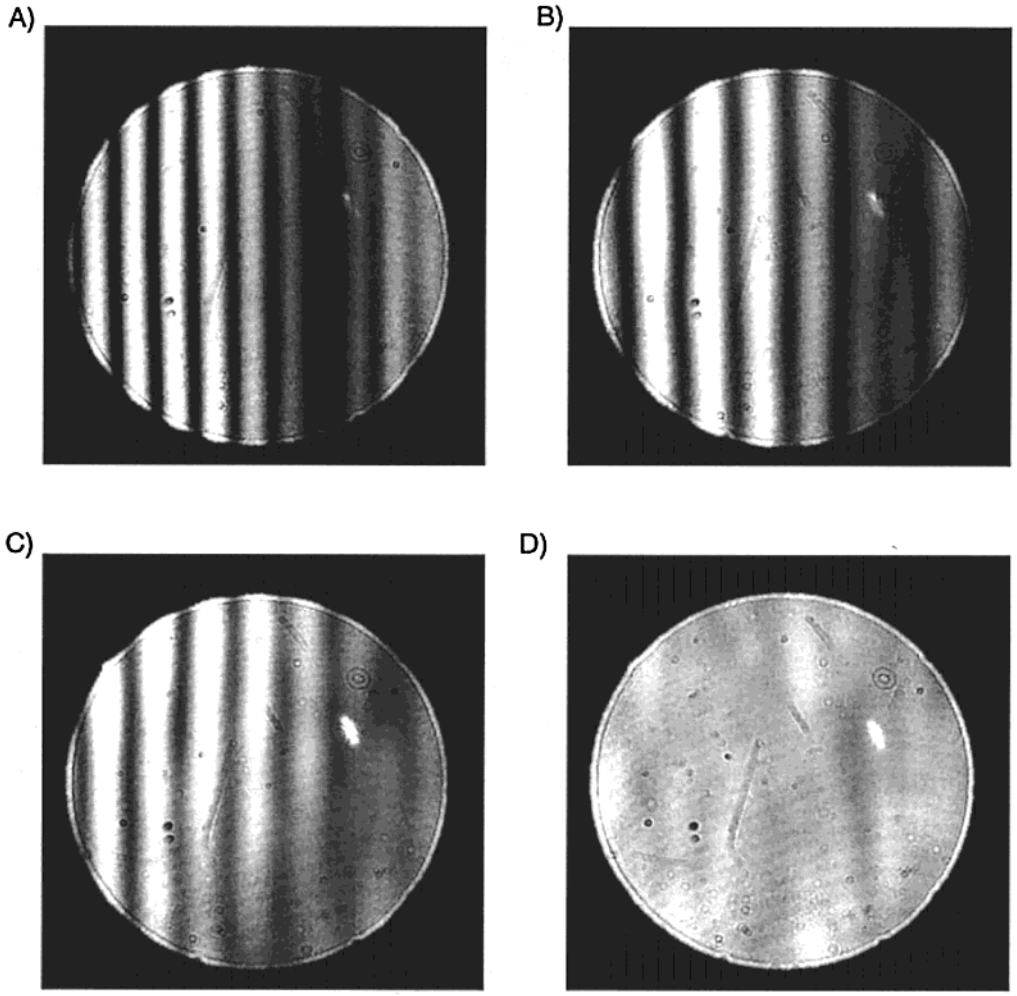

Figure 5. Experimental two-dimensional Fraunhofer diffraction patterns from PEG microparticles doped with TiO_2: (A) polymer-to-ceramic (P/C) weight fraction of 93:1; (B) P/C weight fraction of 13:1; (C) P/C weight fraction of 1:1; (D) P/C weight fraction of 1:8.

depend on the domain parameters. In doing so, we see how coherent interactions between fields scattered by the host and fields scattered by the inclusions result in a dependence on domain parameters that are different from the dependence seen in simple Rayleigh scattering. Here, we provide an overview of the model and an estimate of how the domain-size visibility scales with size and refractive index of the inclusions.

In the VCM, the electric fields scattered at any angle θ, ϕ, are given by

$$\mathbf{E}(\theta,\phi) = \mathbf{E}^{\text{host}}(\theta,\phi) + \mathbf{E}^{\text{i}}(\theta,\phi) \tag{1}$$

where the fields scattered by the host are given by

$$\mathbf{E}^{\text{host}}(\theta,\phi) = E_0 \sum_{v} D_v [f_v^{\text{host}}\ \mathbf{M}_v^{\mathbf{3}}(\theta,\phi) + g_v^{\text{host}}\ \mathbf{N}_v^{\mathbf{3}}(\theta,\phi)] \tag{2}$$

and the fields scattered by the inclusions (in the presence of the host) are given by

$$\mathbf{E}^{\text{i}}(\theta,\phi) = E_0 \sum_{v} D_v [f_v^{\text{i}}\ \mathbf{M}_v^{\mathbf{3}}(\theta,\phi) + g_v^{\text{i}}\ \mathbf{N}_v^{\mathbf{3}}(\theta,\phi)] \tag{3}$$

where the superscript i indicates "inclusion", E_0 is the amplitude of the incident plane wave, $\mathbf{M}_v^{\mathbf{3}}(\theta,\phi)$ and $\mathbf{N}_v^{\mathbf{3}}(\theta,\phi)$ are the vector spherical harmonics for outgoing waves, v is a triple index indicating n, m, and even or odd, and D_v depends only on n and m. The scattering coefficients are f_v^{host} and g_v^{host} for the host and are f_v^{i} and g_v^{i} for the inclusions, where

$$f_v^{\text{i}} = \sum_{j}^{N} f_{v,j}^{\text{i}} \tag{4}$$

and

$$g_v^{\text{i}} = \sum_{j}^{N} g_{v,j}^{\text{i}} \tag{5}$$

where the $f_{v,j}^{\text{i}}$ and $g_{v,j}^{\text{i}}$ are the scattering coefficients for the jth inclusion. There are N inclusions inside the sphere. The total f_v^{i} and g_v^{i} are the sums (the fields add coherently). The relative refractive index is $m_{\text{r}} = n_{\text{incl}}/n_{\text{host}}$, where n_{incl} and n_{host} are the refractive indicies (real parts only) of the inclusion and host, respectively.

The intensity at θ, ϕ is proportional to $\mathbf{E}\cdot\mathbf{E}^*$:

$$|\mathbf{E}^{\text{host}}|^2 + |E_0 \sum_{v} D_v [f_v^{\text{i}}\ \mathbf{M}_v^{\mathbf{3}} + g_v^{\text{i}}\ \mathbf{N}_v^{\mathbf{3}}]|^2 + 2\text{Re}[(\mathbf{E}^{\text{host}})^* E_0 \sum_{v} D_v [f_v^{\text{i}}\ \mathbf{M}_v^{\mathbf{3}} + g_v^{\text{i}}\ \mathbf{N}_v^{\mathbf{3}}]] \tag{6}$$

In a perturbation analysis the second term in eq 6 can be neglected, and eq 6 can be written as

$$|\mathbf{E}^{\text{host}}|^2 + 2\ \text{Re}[(\mathbf{E}^{\text{host}})^* E_0 \sum_{v} D_v (f_v^{\text{i}}\ \mathbf{M}_v^{\mathbf{3}} + g_v^{\text{i}}\ \mathbf{N}_v^{\mathbf{3}})] = I^{\text{host}} + I^{\text{cross}} \tag{7}$$

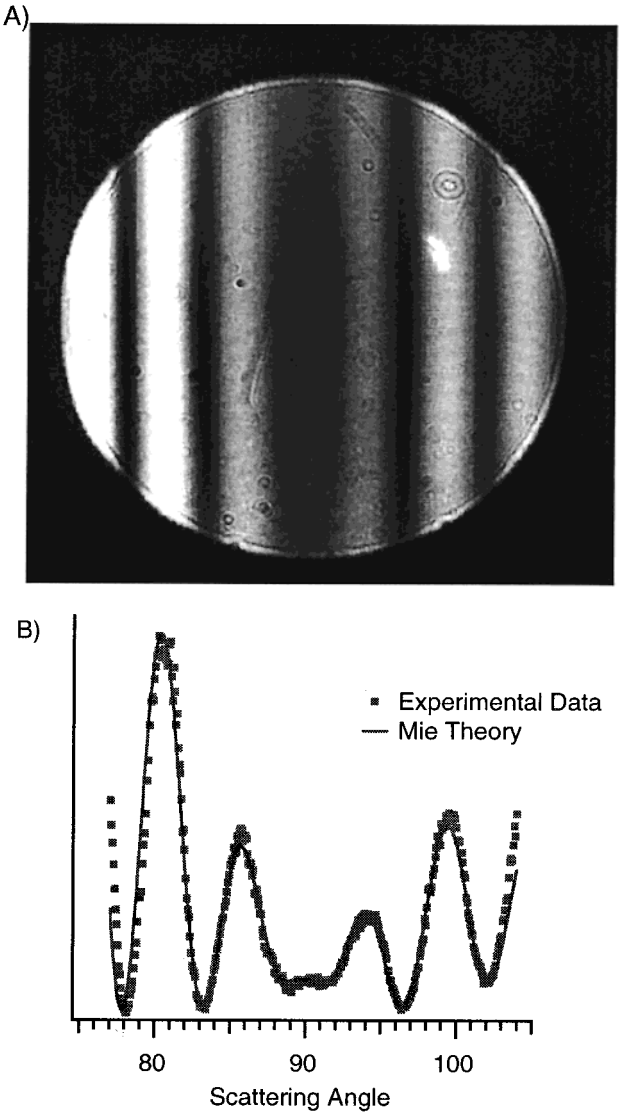

Figure 6. (A) Two-dimensional Fraunhofer diffraction pattern from PEG microparticles doped with carboxylated poly(styrene) latex particles (1:1 weight ratio). (B) 1-D slice of the 2-D pattern (0° polar angle) and Mie theory comparison with the experimental data. The solid line is the experimental data, and the dashed line is the theoretical result for a size 7.268 nm and Re(n) = 1.518.

The angular dependence of the homogeneous sphere is given by I^{host}. We assume the incident plane wave propagates in the z direction, and so only modes with m = 1 are required for the scattering by the homogeneous sphere. The ϕ dependence of these fields is given by cos ϕ and sin ϕ.

The cross term I^{cross} arises from the interactions between $\mathbf{E}^{host}$ and $\mathbf{E}^{i}$. All the m values are required to expand the fields $\mathbf{E}^{i}$ (except in the special case where the inclusions could be confined to the z axis). Deviations from the slowly varying (in ϕ) host fields are caused by modes having m $\neq$ 1. Such fields are responsible for the island structure seen in I^{cross}.

For a host sphere with a fixed size and refractive index, I^{cross} is proportional to

$$\frac{d^3}{\lambda^2}\left|\frac{m_r^2-1}{m_r^2+2}\right| \equiv P \qquad (8)$$

where we used eqs 13, 14, 16, 17, and 29 from ref 27 to obtain f_v^i and g_v^i, along with the far-field expressions for $\mathbf{M}_v^3$ and $\mathbf{N}_v^3$, which are proportional to λ.[30] The parameter P is thus related to the scattering efficiency by size d and the relative refractive index $m = n_{incl}/n_{host}$.

Because I^{cross} is proportional to d^3, the size distribution of subdomains or inclusions may be important. For example, considering only the d^3 term, the scattering efficiency for the 29 nm TiO_2 particles is 8.9 times greater than for the 14 nm polystyrene spheres. However, given the observed number density dependence, contributions from particles that are significantly larger than the average size will be small unless the size distribution is exceedingly broad. I^{cross} is also sensitive to the relative refractive index. In PEG host microspheres (n_{host} = 1.46), the effective scattering by TiO_2 (n_{incl} = 2.5) is 1.8 times greater than equal-sized Al_2O_3 (n_{incl} = 1.7) and 6.7 times greater than equal-sized latex spheres (n_{incl} = 1.59).

It may be surprising that fringe distortion is not observed at a number density of 4×10^4 inclusions when simulations show a clear fringe distortion for 200 inclusions. However, the theory indicates that the scattering intensity of the inclusions scales as the square root of the inclusion number density, which results in an increase in scattering of a factor of 20 when progressing from 100 to 4×10^4 inclusions. The effects of noise and clutter in the experimental method limit the detection efficiency to a level on the order of 10^4 inclusions.

Because the inclusions are at random positions inside the sphere, the total f_v^i and g_v^i (obtained by summing over N inclusions) should be proportional to $\sqrt{N}$. The $f_{v,j}^i$ and $g_{v,j}^i$ for each inclusion have several sources of variation. Because the inclusions are at random positions inside the sphere, their phases are probably random and their magnitudes depend on the strength of the internal electric field at each point and on the coupling between the field point and a source at the inclusion. Therefore, summation over the $f_{v,j}^i$ and $g_{v,j}^i$ is similar to a random walk, where the step sizes are also multiplied by the magnitude of the electric field at that position inside the sphere and by a coupling term (from the Green function relating the inclusion and field points). In the sums to obtain $f_{v,j}^i$ and $g_{v,j}^i$ the dominant contributions will be from inclusions where the internal field $\mathbf{E}$ is large and/or the Green function coupling the inclusion and the field point at θ, ϕ is relatively large.

Although one might think it is best to look for evidence of inclusions in places where I^{host} is smallest (because it is easier to see a small signal against a small "background" than against a large one), I^{cross} is largest where $\mathbf{E}^{host}$ is largest. Therefore, some tricks one might think of to reduce I^{host}, e.g., reducing $\mathbf{E}^{host}$ with a polarizer (because $\mathbf{E}^{i}$ should be depolarized), is not expected to help. Crossed polarizers would, however, be useful for looking for the much smaller term proportional to $|\mathbf{E}^{i}|^2$. The largest term indicating scattering by inclusions, I^{cross}, differs from the largest term for Rayleigh scattering from similar particles in a bulk sample. In that case the scattered intensity from each inclusion is proportional to

$$\left(\frac{d^3}{\lambda^2}\left|\frac{m_r^2-1}{m_r^2+2}\right|\right)^2 \qquad \text{[ref 9, p 132]}$$

which is proportional to the square of the term proportional to I^{cross}. If crossed polarizers were used to minimize $\mathbf{E}^{host}$ at some positions, then the remaining intensity coming from scattering by the inclusions would be proportional to the Rayleigh term. Whether I^{cross} can be detected against the background I^{host} depends on the noise in the measurement.

Summary

We have studied experimentally the domain size, refractive index, and number density dependence of nanometer-sized guest particles doped into PEG host microparticles using 2-D optical diffraction. This work was motivated by a need for a more quantitative understanding of the relationships between material homogeneity on length scales between 10 and 50 nm and distorted 2-D diffraction (scattering) patterns from spherical host microparticle, issues that are relevant to characterizing material homogeneity in polymer blend microparticles. We find that for both Al_2O_3 and TiO_2 ceramic nanoparticles (sizes 29 and 46 nm, respectively) doped into PEG host microparticles, material heterogeneity is manifested in distorted angular scattering patterns with a guest/host weight ratio threshold of $\geq 8\%$. Results of theoretical modeling indicate that considerably lower densities of guest inclusions could be observed by reducing the experimental noise. For smaller latex particle dopants (14 nm), the composite microparticles appear homogeneous even at unit relative host/guest weight fractions. Depending on the difference in refractive index between the host and guest, and the choice of probe wavelength, these results show that the domain-size threshold for fringe distortion in our experiments, proportional to

$$\sqrt{N}\frac{d^3}{\lambda^2}\left|\frac{m^2-1}{m^2+1}\right|$$

is about 30 nm. Thus, we have demonstrated rigorously that this technique is capable of providing information on material homogeneity at length scales comparable to macromolecular dimensions.

Acknowledgment. This research was sponsored by the U.S. Department of Energy, Office of Basic Energy Sciences (Divisions of Chemical Sciences and Materials Sciences) under Contract DEAC05-96OR22464 with Oak Ridge National Laboratory managed by Lockheed Martin Energy Research Corporation. J.V.F acknowledges support from the ORNL Postdoctoral Research Associates Program administered by Oak Ridge Associated Universities.

References and Notes

(1) Jenekhe, S. A.; Zhang, X. J.; Chen, X. L.; Choong, V. E.; Gao, Y. L.; Hsieh, B. R. *Chem. Mater.* **1997**, *9*, 409.

(2) Croce, F.; Appetecchi, G. B.; Persi, L.; Scrosati, B. *Nature* **1998**, *394*, 456.

(3) Weston, J. E.; Steele, B. C. H. *Solid State Ionics* **1982**, *7*, 75.

(4) Barnes, M. D.; Kung, C.-Y.; Fukui, K.; Sumpter, B. G.; Noid, D. W.; Otaigbe, J. U. *Opt. Lett.* **1999**, *24*, 121.

(5) Barnes, M. D.; Ng, K. C.; Fukui, K.; Sumpter, B. G.; Noid, D. W. *Macromol.* **1999**, *32*, 7183.

(6) Kung, C.-Y.; Barnes, M. D.; Lermer, N.; Whitten, W. B.; Ramsey, J. M. *Anal. Chem.* **1998**, *70*, 685.

(7) Ford, J. V.; Sumpter, B. G.; Noid, D. W.; Barnes, M. D. Observation of Size Oscillations in Poly(ethylene) Glycol/Electrolyte Composite Microparticles. *Chem. Phys. Lett.*, in press.

(8) Holler, S.; Pan, Y.; Chang, R. K.; Bottiger, J. R.; Hill, S. C.; Hillis, D. B. *Opt. Lett.* **1998**, *23*, 1489.

(9) Bohren, C. F.; Huffman, D. R. *Absorption and Scattering of Light by Small Particles*; Interscience: New York, 1983.

(10) Ashkin, A.; Dziedzic, J. M. *Phys. Rev. Lett.* **1977**, *38*, 1351.

(11) Ashkin, A.; Dziedzic, J. M. *Appl. Opt.* **1981**, *20*, 1803.

(12) Arnold, S.; Folan, L. M. *Rev. Sci. Instrum.* **1986**, *57*, 2250.

(13) Davis, E. J.; Ray, A. K. *J. Colloid Interface Sci.* **1980**, *75*, 566.

(14) Hill, S. C.; Benner, R. E. *Optical Effects Associated with Small Particles*; Barber, P. W., Chang, R. K., Eds.; World Scientific: Singapore, 1988; Chapter 1.

(15) Eversole, J. D.; Lin, H. B.; Huston, A. L.; Campillo, A. J. *J. Opt. Soc. Am. A* **1990**, *7*, 2159.

(16) Owen, J. F.; Barber, P. W.; Messinger, B. J.; Chang, R. K. *Opt. Lett.* **1981**, *6*, 272.

(17) Eversole, J. D.; Lin, H. B.; Huston, A. L.; Campillo, A. J.; Leung, P. T.; Liu, S. Y.; Young, K. *J. Opt. Soc. Am. B* **1993**, *10*, 1955.

(18) Barnes, M. D.; Kung, C.-Y.; Whitten, W. B.; Ramsey, J. M.; Arnold, S.; Holler, S. *Phys. Rev. Lett.* **1996**, *76*, 3931.

(19) Thurn, R.; Kiefer, W. *Appl. Opt.* **1985**, *24*, 1515.

(20) Snow, J. B.; Qian, S.-X.; Chang, R. K. *Opt. Lett.* **1985**, *10*, 37.

(21) *Optical Processes in Microcavities*; Chang, R. K., Campillo, A. J., Eds.; World Scientific: Singapore, 1997.

(22) Arnold, S.; Folan, L. M. *Opt. Lett.* **1989**, *14*, 387.

(23) Ray, A. K.; Souyri, A.; Davis, E. J.; Allen, T. M. *Appl. Opt.* **1991**, *30*, 3974.

(24) Kung, C.-Y.; Barnes, M. D.; Lermer, N.; Whitten, W. B.; Ramsey, J. M. *Appl. Opt.* **1999**, *38*, 1481.

(25) Barnes, M. D.; Lermer, N.; Whitten, W. B.; Ramsey, J. M. *Rev. Sci. Instrum.* **1997**, *68*, 2291.

(26) For large macromolecules, MW $> 10^5$, molecular radii are about 20 nm.

(27) Hill, S. C.; Salaheen, H. I.; Fuller, K. A. *J. Opt. Soc. Am. A* **1995**, *12*, 905.

(28) Bronk, B. V.; Smith, M. J.; Arnold, S. *Opt. Lett.* **1993**, *18*, 93.

(29) van de Hulst, H. C. *Light Scattering by Small Particles*; John Wiley & Sons: New York, 1957; p 70.

(30) Note that although there is a reciprocal size parameter (which is proportional to wavelength) on the right-hand side of eqs 13 and 14 of the VCM paper, the large-scale trend of the complete fractions (which multiply the c_v^H and d_v^H) is to neither increase nor decrease with wavelength (these fractions have resonance oscillations, but we are concerned with the values averaged over a wavelength range).